

## Optimal design of microscaled scattering optical elements

Andreas Håkansson and José Sánchez-Dehesa<sup>a)</sup>

Wave Phenomena Group, Nanophotonic Technology Center, Polytechnic University of Valencia,  
C/ Camino de Vera s/n, E-46022, Valencia, Spain

(Received 16 March 2005; accepted 9 September 2005; published online 2 November 2005)

A method of inverse design is applied to generate an optical device that acts as a wavelength demultiplexer. The ultracompact device, only  $2\ \mu\text{m}$  thick, is designed to separate two wavelengths  $1.55\ \mu\text{m}$  and  $1.50\ \mu\text{m}$ , respectively, and consists of five layers of  $0.4\ \mu\text{m} \times 0.4\ \mu\text{m}$  square-shaped bars etched in gallium arsenide. The expected cross talk is suppressed below  $-25\ \text{dB}$  for both wavelengths. The proposed device is an example of a scattering optical element, a name here introduced to define a class of computer-generated optical devices and whose functionalities are based on the multiple scattering by their individual constituents. For realization of the aforementioned devices, two-dimensional photonic plates can be prepared by only a single integrated circuit processing procedure followed by micromanipulation assembling. © 2005 American Institute of Physics. [DOI: 10.1063/1.2126134]

Diffractive optical elements<sup>1,2</sup> (DOEs) are optical devices that solve the inverse problem of shaping a laser beam to practically any projection pattern. Because of this feature, DOEs are currently used in a wide range of applications such as lenses, deflectors, LED collimators, or fan-out elements. DOEs can tailor practically any specific intensity pattern by controlling the phase of scattered waves. This is normally achieved by assembling a layer of smaller elements, where each element manipulates one part of the incident beam. The elements are fabricated by controlling their thicknesses and/or refractive index parameters, which are computer generated through optimization to forge the beam that propagates through the layer into the desired shape.

Here, another class of optical devices that are named scattering optical elements (SOEs) are proposed for molding the flow of light. Instead of using a single layer of phase-controlling components, as DOEs, SOEs are based on the multiple scattering by a few layers of individual scatterers, whose positions and shapes are inverse designed to accomplish a given functionality. Since we acquire a new freedom of the third dimension through SOEs, we can shape the fields with vast controllability. Additionally, because SOEs are porous, the reflection can be controlled from totally opaque, similar to a Bragg reflector, to almost completely transparent, a possibility of light control that is not possible using conventional DOEs.

This letter presents a wavelength demultiplexer as an example of a SOE designed with a prefixed functionality. This optical element is used to achieve wavelength-division multiplexing (WDM) that increases local area network bandwidth in optical communication. WDMs use optical multiplexers and demultiplexers (DEMUX) to simultaneously route different information channels through an optical network. An approach toward microscale WDMs has been proposed by Noda *et al.*,<sup>3</sup> who produced add/drop filters by using the trapping and emission of photons by isolated defects integrated with a photonic crystal (PhC) waveguide. A different approach reported by Kosaka *et al.*<sup>4</sup> consists of taking advantage of the nonlinear dispersion relation of PhC to

achieve extremely wavelength-dependent light steering. An angle dispersion of  $50^\circ$  for a 1% change in the wavelength was reported. In this letter, an ultracompact DEMUX is here designed to separate two specific wavelengths,  $\lambda_1 = 1.55\ \mu\text{m}$  and  $\lambda_2 = 1.50\ \mu\text{m}$ , where the angle separation equals  $28^\circ$  and both crosstalks are suppressed under  $-25\ \text{dB}$ .

Figure 1 shows a schematic view of how the optical DEMUX operates over the incoming light beam together with the parameters involved in the process of inverse design. In particular,  $x_f$  defines the distance to the plane where the split-up beams are forced to adopt a given position and width,  $d$  and  $2\epsilon$ , respectively.

The process of designing a SOE requires a fast and accurate simulation method, to solve the direct scattering problem, and a competent global optimization algorithm. First, to solve Maxwell's equations in a system of two-dimensional (2D) dielectric scatterers, the multiple scattering theory (MST) is employed because of its efficiency and accuracy when dealing with a reasonable number of scatterers. For example, to simulate the scattering of light by a cluster of

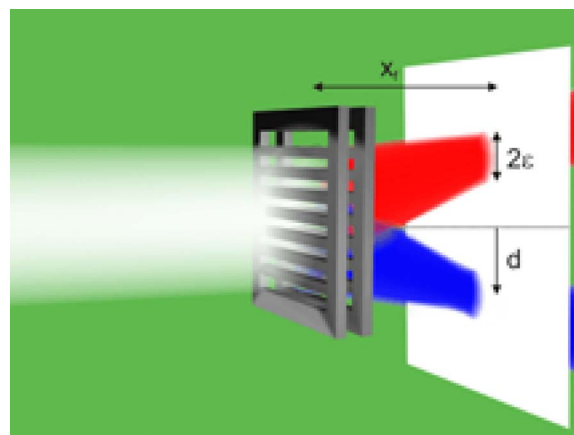


FIG. 1. (Color online) Schematic view of the functionality of a demultiplexer based on a scattering optical element (SOE) consisting of two layers of dielectric rectangular bars on air. The three lengths in this plots ( $x_f$ ,  $d$ , and  $\epsilon$ ) are parameters in the process of inverse design (see text). The white plane defines the position where the signal is captured.

<sup>a)</sup>Electronic mail: jsdehesa@upvnet.upv.es

100 dielectric rods takes only a few seconds on a normal Pentium IV home computer. Second, the genetic algorithm (GA) is chosen as the optimization method since it has been proved to be effective in finding the global optimum of complex problems in photonics,<sup>5-8</sup> though basically any search algorithm could be used in the inverse design process. The GAs often need to calculate many configurations before converging, but the use of MST makes such calculations possible in a reasonable CPU time. The combination MST-GA is a powerful tool for inverse design. However, both methods have been employed with a few simplifications. Thus, with respect to the MST, the calculation of the  $T$ -matrix<sup>9</sup> has been reduced to scatterers with equal square cross sections. With regards to the Georgia, the optimization is carried out under the assumption that all the scatterers have a fixed position, hence a one-bit parameter codes the presence or absence of each scatterer. For technical details about how the MST-GA is implemented, the reader should review previous works, where this inverse design tool has been successfully applied to generate different photonic<sup>10,11</sup> and phononic<sup>7,8</sup> devices.

A promising method to fabricate a real three-dimensional (3D) SOE structure, consists of slicing the total structure into several 2D photonic plates prepared by a semiconductor nanofabrication technique. Subsequently, these plates are assembled into the 3D structure by micromanipulation.<sup>12,13</sup> The inverse design is carried out under the constraints of this specific fabrication method. Only five layers of 2D photonic plates are assumed to form the photonic device; this to guarantee that a perfect alignment of these layers will be possible by the micromanipulation technique. The dielectric constant of the rods is considered to be that of gallium arsenide (GaAs) at the wavelength of interest ( $\sim 1.50 \mu\text{m}$ ),  $\epsilon_{\text{GaAs}} \approx 11.36$ .

The rods have all equal square cross sections, measuring  $0.4 \mu\text{m} \times 0.4 \mu\text{m}$ , and are positioned into a fixed set of lattice points. Because of the thickness of  $0.4 \mu\text{m}$  of a planar unit, the total thickness of the SOE-DEMUX device will be  $2 \mu\text{m}$ . The separation,  $x_f$ , between the SOE and the plane where the signal will be captured (see Fig. 1) is set to  $20 \mu\text{m}$ . In order to avoid cross talk between  $\lambda_1$  and  $\lambda_2$  the space separation,  $2d$ , has been set to  $10 \mu\text{m}$ . Furthermore, it is assumed that the minimal area for the signal capture,  $2\epsilon$ , is approximately  $2 \mu\text{m}$ . Finally, the incident laser beam was simulated as Gaussian shaped having a width of  $10 \mu\text{m}$  and polarized so the electric field oscillates parallel to the central axis of the rods. Using these parameters, the fitness function for the DEMUX device is chosen as,

$$f(\vec{s}) = 20 \log \left( \frac{\int_{-d-\epsilon}^{-d+\epsilon} |E_z(x_f, y)|_{\lambda_1} dy \cdot \int_{-d-\epsilon}^{-d+\epsilon} |E_z(x_f, y)|_{\lambda_2} dy}{\int_{-d-\epsilon}^{-d+\epsilon} |E_z(x_f, y)|_{\lambda_2} dy \cdot \int_{-d-\epsilon}^{-d+\epsilon} |E_z(x_f, y)|_{\lambda_1} dy} \right), \quad (1)$$

where  $\vec{s}$  is the digital string that includes the digital parameters for coding the SOE. This function corresponds to the summation of the cross-talk attenuation, in decibels, for the two wavelength channels. Now, maximizing  $f(\vec{s})$  will guarantee a minimal cross talk between  $\lambda_1$  and  $\lambda_2$  at the coordinates  $(x_f, d)$  and  $(x_f, -d)$  and for a resolution  $2\epsilon$ .

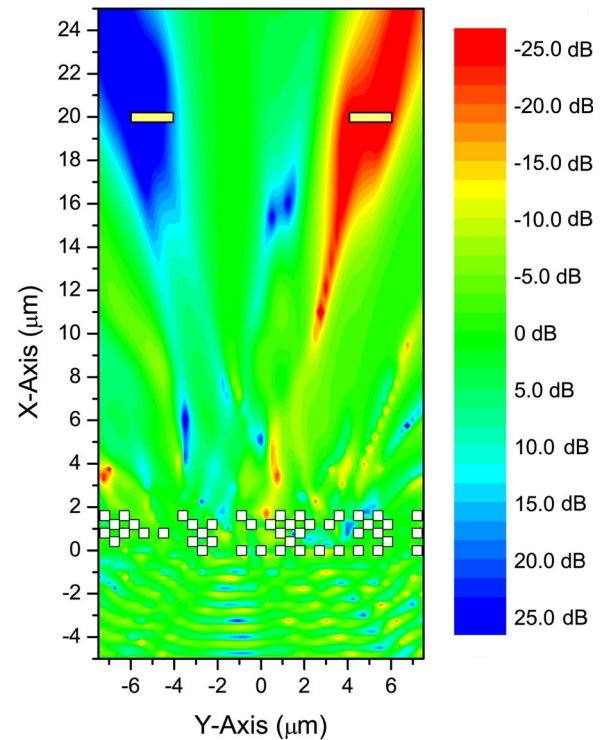


FIG. 2. (Color online) The optimized DEMUX-SOE device computer generated by our algorithm of inverse design is represented by the set of white squares at the region  $0 \leq x \leq 2 \mu\text{m}$ . The map prints out the function  $-20 \log[|E_z(x, y)|_{\lambda=1.55 \mu\text{m}} / |E_z(x, y)|_{\lambda=1.50 \mu\text{m}}]$  produced by an incident Gaussian beam travelling in the positive  $x$  direction. The yellow rectangles define geometrical parameters used in the optimization procedure.

Notice that although the design procedure uses a 2D simulation method for fast simulations reasons, the resulting device is expected to represent an actual 3D device as it has been successfully demonstrated in its acoustical counterpart.<sup>8</sup>

To codify the five-layer SOE, 85 lattice positions are used in the optimization process (17 for layers 1, 3, and 5, and 16 for layers 2 and 4). The specific lattice positions result in 85 binary variables that give rise to a total number of  $3.9 \times 10^{25}$  configurations. The inverse design was performed under the constraints set above by maximizing the fitness function defined in Eq. (1). The maximum value  $f(\vec{s}) = 52.7$  was found after 20 000 configuration evaluations, equaling approximately 45 h using a Pentium IV processor. The final device is shown in Fig. 2. This map prints out  $-20 \log(|E_z(x, y)|_{\lambda_1} / |E_z(x, y)|_{\lambda_2})$ , i.e., the predicted cross talk between the two wavelengths. It can be seen that an attenuation of 25 dB is achieved for the desired coordinates, marked with a yellow box in the figure. In more detail, Fig. 3 shows the electric field amplitude for the two different frequencies and for a cross section at  $x_f = 20 \mu\text{m}$ . In comparison with the alternative design reported in Ref. 4 this chosen angular dispersion is inferior. However, our device is two orders of magnitude smaller. Let us also stress that other solutions, with a similar performance, could be obtained by modifying the setup of the problem; the number of rods, their positions and shape, the material, etc.

In summary, scattering optical elements based on a few planar components, each one prepared using conventional integrated circuit processing procedure with subsequent assembly into 3D structure by micromanipulation, are proposed as photonic devices for molding the flow of light.

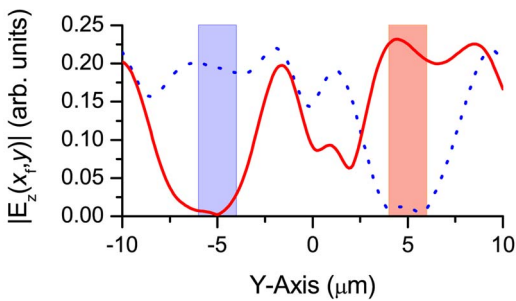


FIG. 3. (Color online) Electric field modulus,  $|E_z(x_f, y)|$ , for the two wavelengths  $1.55 \mu\text{m}$  (red solid line) and  $1.50 \mu\text{m}$  (blue dotted line) calculated at the distance  $x_f$  from the DEMUX device (see Fig. 1). The rectangles define geometrical parameters used in the optimization procedure.

Here, an optical DEMUX is computer generated by a MST-GA inverse design tool, which has been applied with the constraints that makes its experimental fabrication and characterization feasible at the micro scaled regime.

The authors acknowledge Hideki T. Miyazaki and Kanna Aoki for suggesting this problem to us and for their valuable help in defining the parameters of the device for its practical realization. The financial support provided by the Spanish

Ministry of Education and Science (MEC) (Contract Nos. TEC2004-02345 and NAN2004-08843), Comunidad Autónoma de Madrid (GR/MAT/0729/2004), and the Nanophotonic Technology Center of Valencia are gratefully acknowledged.

- <sup>1</sup>L. B. Lesem, P. M. Hirsch, and J. J. A. Jordan, *IBM J. Res. Dev.* **13**, 150 (1969).
- <sup>2</sup>J. L. Horner and P. D. Gianino, *Appl. Opt.* **23**, 812 (1984).
- <sup>3</sup>S. Noda, A. Chutinan, and M. Imada, *Nature (London)* **407**, 608 (2000).
- <sup>4</sup>H. Kosaka, T. Kawashima, A. Tomita, M. Notomi, T. Tamamura, T. Sato, and S. Kawakami, *Appl. Phys. Lett.* **74**, 1370 (1999).
- <sup>5</sup>S. Preble, M. Lipson, and H. Lipson, *Appl. Phys. Lett.* **86**, 061111 (2005).
- <sup>6</sup>M. Spuhler, B. Offrein, G. Bona, R. Germann, I. Masserek, and D. Erni, *J. Lightwave Technol.* **16**, 1680 (1998).
- <sup>7</sup>A. Håkansson, L. Sanchis, and J. Sánchez-Dehesa, *Phys. Rev. B* **70**, 214302 (2004).
- <sup>8</sup>A. Håkansson, F. Cervera, and J. Sánchez-Dehesa, *Appl. Phys. Lett.* **86**, 054102 (2005).
- <sup>9</sup>P. Waterman, *Phys. Rev. D* **3**, 825 (1971).
- <sup>10</sup>L. Sanchis, A. Håkansson, D. Lopez-Zanón, J. Bravo-Abad, and J. Sánchez-Dehesa, *Appl. Phys. Lett.* **84**, 4460 (2004).
- <sup>11</sup>A. Håkansson, J. Sánchez-Dehesa, and L. Sanchis, *IEEE J. Sel. Areas Commun.* **23**, 1365 (2005).
- <sup>12</sup>K. Aoki, H. T. Miyazaki, H. Hirayama, K. Inoshita, T. Baba, N. Shinya, and Y. Aoyagi, *Appl. Phys. Lett.* **81**, 3122 (2002).
- <sup>13</sup>K. Aoki, H. T. Miyazaki, H. Hirayama, K. Inoshita, T. Baba, N. Shinya, and Y. Aoyagi, *Nat. Mater.* **2**, 117 (2003).